Hindawi
Oxidative Medicine and Cellular Longevity
Volume 2019, Article ID 2593742, 13 pages
https://doi.org/10.1155/2019/2593742

Research Article

Acetaldehyde Induces Neurotoxicity *In Vitro* via Oxidative Stress- and Ca^{2+} Imbalance-Mediated Endoplasmic Reticulum Stress

Jiahui Cui, Yang Liu, Xing Chang, Wenfeng Gou, Xuejiao Zhou, Zi Liu, Zengqiang Li, Yingliang Wu, and Daiying Zuo

Shenyang Pharmaceutical University, 103 Wenhua Road, Shenyang, Liaoning 110016, China

Correspondence should be addressed to Yingliang Wu; yingliang_1016@163.com and Daiying Zuo; zuodaiying@163.com

Received 8 May 2018; Accepted 13 November 2018; Published 9 January 2019

Academic Editor: Andrey V. Kozlov

Excessive drinking can damage brain tissue and cause cognitive dysfunction. Studies have found that the early stage of neurodegenerative disease is closely related to heavy drinking. Acetaldehyde (ADE) is the main toxic metabolite of alcohol. However, the exact mechanisms of ADE-induced neurotoxicity are not fully clear. In this article, we studied the cytotoxic effect of ADE in HT22 cells and primary cultured cortical neuronal cells. We found that ADE exhibited cytotoxicities against HT22 cells and primary cultured cortical neuronal cells in dose-dependent manners. Furthermore, ADE induced apoptosis of HT22 cells by upregulating the expression of caspase family proapoptotic proteins. Moreover, ADE treatment could significantly increase the intracellular Ca^{2+} and reactive oxygen species (ROS) levels and activate endoplasmic reticulum stress (ERS) in HT22 cells. ADE upregulated ERS-related CHOP expression dose-dependently in primary cultured cortical neuronal cells. In addition, inhibition of ROS with antioxidant N-acetyl-L-cysteine (NAC) reduced the accumulation of ROS and reversed ADE-induced increase of ERS-related protein and apoptosis-related protein levels. Mitigation of ERS with ERS inhibitor 4-PBA obviously suppressed ADE-induced apoptosis and the expression of ERS-related proteins. Therefore, ADE induces neurotoxicity of HT22 cells via oxidative stress- and Ca^{2+} imbalance-mediated ERS.

1. Introduction

Alcohol abuse and alcoholism have become severe social problems. Excessive alcohol consumption can not only lead to extensive tissue damage in organs such as the brain, heart, and liver but also promote disease states, including diabetes mellitus and neuropsychiatric disorders such as Alzheimer's disease [1]. The brain is one of the major targets of alcohol actions. Alcohol-induced brain damage can produce some potential effects of alcoholism, including cognitive disorders such as learning and memory impairment [2].

The major alcohol metabolites are acetaldehyde (ADE) and acetate, and ADE plays a key role in alcohol-induced neurotoxicity [3]. The conventional view believes that the oxidation of alcohol to ADE can occur in the brain through pathways that involve enzymes including alcohol dehydrogenases (ADHs), catalase, and cytochrome P4502E1 [4]. ADE is catalyzed by acetaldehyde dehydrogenase (ALDH) and is metabolized into acetate with the help of P4502E1. The final metabolites of acetate are carbon dioxide and water [5]. For ALDH, there are three isozymes including ALDH1, ALDH2, and ALDH3. The conversion of ADE was mainly performed by ALDH2 in the mitochondria of hepatocytes [3]. It has been found that the levels of ADE in the blood of individuals with defective ALDH2 are much higher in comparison with those of normal individuals after alcohol ingestion [6]. Unfortunately, 30% to 40% of Asians are deficient in ALDH, resulting in a large accumulation of ADE in the body which cannot be metabolized, so compared to alcohol, ADE may cause greater damage to the human body [7]. Some recent

evidences prove that some of the *in vivo* and *in vitro* effects of alcohol are mediated by ADE, which may be a crucial factor in the central effects of alcohol [8–10]. Although there are some advancements in the understanding of ADE's central effects in recent years [4, 11], the exact mechanism underling ADE's effects remains largely unknown.

ADE has been proved contributing to many adverse effects of alcohol [12]. Significant behavioral evidences implicate that ADE is involved in the psychopharmacological effects of alcohol [13–15]. At low concentrations, ADE induces euphoria [16] and has been involved in alcohol addiction [17, 18]. In fact, people can be exposed to ADE in their daily lives via different routes, including alcoholic beverages, tobacco smoke, and food additives and fragrances [19]. ADE can damage protein and lipid functions, resulting in DNA damage and mutation [20] and increase of reactive oxygen species (ROS) [21], leading to extensive impairments of protein function, gene expression, and DNA integrity [22, 23]. Although numerous researches have focused on the role of ADE in different aspects of alcohol effects, there is little study that relates ADE to neurotoxicity. In particular, the action mechanism of ADE is still not fully understood.

Endoplasmic reticulum stress (ERS) resulting from accumulation of unfolded and misfolded proteins within endoplasmic reticulum (ER) lumen has been reported to account for the neuronal death induced by cerebral ischemia, hypoxia, and trauma [24, 25]. ERS and unfolded protein response (UPR) are mediated by three transmembrane ER signaling proteins: pancreatic endoplasmic reticulum kinase (PERK), inositol-requiring enzyme 1 (IRE1), and activating transcription factor 6 (ATF6) [26]. Further, ER is closely related to the redox reaction of the energy center mitochondria, leading to an inseparable relationship between ERS and oxidative stress [27]. In addition, studies suggest that ERS may play an important role in alcohol-induced brain damage [28, 29]. Various stimuli disrupting the homeostasis of cells can cause abnormal protein loading and modification of ER [26]. However, the role of ERS in ADE-induced neurotoxicity remains unclear.

In this study, we investigated the cytotoxic effect of ADE in mouse hippocampal HT22 cells and primary cultured cortical neuronal cells and explored the relationship between ERS and ADE-induced neurotoxicity. We found that ADE induced apoptosis of HT22 cells by upregulating the expression of cleaved caspase-3, cleaved caspase-9, and cleaved caspase-12. ADE treatment led to significant activation of ERS and ROS. In addition, inhibition of ROS with antioxidant N-acetyl-L-cysteine (NAC) and mitigation of ERS with ERS inhibitor sodium phenylbutyrate (4-PBA) obviously suppressed ADE-induced apoptosis and the expression of ERS-related proteins.

2. Experimental Materials and Methods

2.1. Materials and Reagents. ADE with 40% purity was obtained from BBI Life Sciences (Shanghai, China). Dulbecco's modified Eagle's medium (DMEM)/F12, B27 supplement, fetal bovine serum (FBS), and DMEM were obtained from Gibco (USA). Annexin V-FITC/PI double-staining and TUNEL Apo-Green detection kits were purchased from BioTools, Inc. (Houston, TX, USA). MTT, acridine orange/ethidium bromide (AO/EB), and 4,6-diamino-2-phenolindol dihydrochloride (DAPI) were from Sigma (USA). Ca^{2+} kit, 2′,7′-dichlorodihydrofluorescein diacetate (DCFH-DA), and NAC were from Beyotime (Nanjing, China). 4-PBA was purchased from Selleckchem (Houston, TX, USA). Bovine serum albumin (BSA) was from Biosharp (Hefei, China). Rabbit anti-CHOP, anti-GRP78, anti-ATF6, anti-PERK, anti--p-PERK, anti-IRE1, and anti-p-IRE1 IgG were purchased from Bioss (Beijing, China). Rabbit anti-cleaved capase-9 and anti-cleaved caspase-12 IgG were from Proteintech (Wuhan, China) and Santa Cruz Biotechnology (USA), respectively. Rabbit anti-Bax, anti-Bcl-2, horseradish peroxidase-conjugated, and FITC-conjugated secondary antibodies were from Santa Cruz Biotechnology (USA). Rabbit anti-cleaved caspase-3 was obtained from Cell Signaling Technology (USA). βIII-tubulin was from Sigma (USA). TRIzol reagent Qiagen was purchased from Qiagen (Germany). HiFiScript cDNA synthesis kit and GreenStar qPCR master mix were obtained from Cwbio (China) and Bioneer (South Korea), respectively.

2.2. HT22 Cell Cultures. Mouse hippocampal neuron HT22 cell line was obtained from JENNIO Biological Technology (Guangzhou, China). HT22 cells were cultured in DMEM complemented with 10% FBS, 100 mg/ml streptomycin, and 100 U/ml penicillin and were maintained in a humidified incubator at 37°C and 5% CO_2. For each experiment, cells were plated until 70–80% confluence and digested with trypsin.

2.3. Primary Culture of Rat Cortical Neuronal Cells. Primary cultured neurons were prepared as previously described [30]. Neuronal cultures were prepared from the cerebral cortex of neonatal Sprague-Dawley rats of postnatal day 1. Animal procedures were designed to minimize the number of animals required, and appropriate steps were taken to avoid unjustified animal procedures and discomfort. After rats were terminated, their brains were quickly removed and cerebral cortices were dissected in ice-cold DMEM/F12 solution. Subsequently, neurons were dissociated and suspended in complete medium containing DMEM/F12, 15% FBS, 100 U/ml penicillin, and 100 U/ml streptomycin sulfates and counted in a hemocytometer. Approximately 10^6 cells/ml per well were plated on poly-D-lysine-coated 48-well plates in medium according to different experimental requirements and cultured in the incubator with 5% CO_2 at 37°C. Neuronal cell culture medium was changed with serum-free DMEM/F12+2% B27 supplement at 48 h; subsequently, half of the cell culture medium was replaced every 48 h. On the 4th day, cultures were fed with medium containing Ara-C (2.5 mg/ml) for 2 days to prevent growth of glial cells. The neurons were cultured 6 days for experimental use.

2.4. MTT Colorimetric Assay. Cell viability was determined by routine MTT assays [30]. Cell growth inhibition percentage was calculated by SPSS 22.0 software.

2.5. Cell Morphology Changes. 2×10^5 cells were seeded per well in a 6-well plate and incubated with ADE for 24 h, and the cells were photographed by an optical microscope (Olympus, Tokyo, Japan). Morphological changes of nuclei after staining with Hoechst 33258 solution for 20 min were observed by fluorescence microscopy (Olympus, Tokyo, Japan).

2.6. Detection of Apoptotic Cells. 2×10^5 cells were seeded per well in a 6-well plate and incubated with ADE for 24 h, then the cells were stained with AO/EB mixed solution 20 μl (AO : EB = 1 : 1). The morphological changes of the cells were observed with a fluorescence microscope (Olympus, Tokyo, Japan).

2.7. Apoptosis Analysis. HT22 cells were incubated with various doses of ADE for 24 h, then the cells were washed three times with PBS and stained with Annexin V-FITC and PI at 20–25°C for 20 min. Then, the apoptosis rates were measured by FACScan flow cytometry (Becton Dickinson, Franklin Lakes, NJ, USA).

2.8. Intracellular Ca^{2+} Measurement. In HT22 cells, fluo-4/acetoxymethyl ester (AM) can be deacetylated to fluo-4, and fluo-4 can bind to intracellular Ca^{2+} to increase green fluorescence, so intracellular Ca^{2+} levels were detected by fluo-4/AM. After treatment with ADE, cells were incubated with 1 ml fluo-4/AM solution (10 mg/ml) for 30 min at 37°C. Microscopic images were obtained by a confocal microscopy (Nikon C2, Tokyo, Japan). ImageJ software was used to measure the fluorescence intensity.

2.9. Intracellular ROS Measurement. ROS level was assessed by DCFH-DA staining according to previous methods [30].

2.10. ER Structure Observation by Transmission Electron Microscopy (TEM). After being treated with ADE (1.25 mM) for 24 h, HT22 cells were digested with trypsin and fixed with 2.5% glutaraldehyde. Then, ultrathin sections (1 μm) were observed by TEM (Hitachi, Tokyo, Japan).

2.11. Quantitative Real-Time PCR (RT-PCR). RT-PCR was performed following a routine procedure. Total RNA was extracted from HT22 cells with TRIzol reagent according to the manufacturer's instructions. The primer sequences were as follows.

(i) GRP78: 5′-GAAGGAGGATGTGGGCACG-3′ and 5′-CGCATCGCCAATCAGACG-3′

(ii) PERK: 5′-CCGCAAGAAGGACCCTATCC-3′ and 5′-GAGTTTCAGACTCCTTCCGCT-3′

(iii) ATF6: 5′-ACCTGTTCTTCCTCTGAAATCCAA-3′ and 5′-AGGACAGAGAAACAAGCTCGG-3′

(iv) Caspase-12: 5′-TGGAAGGTAGGCAAGACT-3′ and 5′-ATAGTGGGCATCTGGGTC-3′

(v) CHOP: 5′-AGTCCCTGCCTTTCACCTT-3′ and 5′-GCTTTGGGATGTGCGTGTG-3′

(vi) GAPDH: 5′-GTATGACTCCACTCACGGCAA-3′ and 5′-CACCAGTAGACTCCACGACA-3′

2.12. Immunofluorescence Staining. The primary cultured neuron cells were seeded into six-well plates with cover glasses in each well and then treated with ADE and medium for 24 h. Immunofluorescence analysis was performed as previously described to determine βIII-tubulin and CHOP [30].

2.13. Western Blotting Analysis. After collecting ADE-treated HT22 cells, the proteins of the cells were extracted and the protein contents of the isolated supernatant were determined by a protein assay reagent. Equivalent amounts of protein (40 mg) were separated by gel electrophoresis. Then, the protein was transferred to a polyvinylidene difluoride (PVDF) membrane (Millipore Bedford, MA, USA). The membranes were immersed in 5% skimmed milk. Then, the primary antibodies were incubated with target antigens at 4°C overnight. The next day, horseradish peroxidase- (HRP-) conjugated secondary antibodies (1 : 3000) were incubated with the target antigens for 2 h. The enhanced chemiluminescence was used to visualize the proteins, and ImageJ software was used to do the densitometry analysis.

2.14. Statistical Analysis. Data were expressed as the mean ± SD of at least three representative experiments. Statistical significance was assessed using SPSS software 19.0 by one-way analysis of variance (ANOVA), followed by Dunnett's multiple comparison tests. A p value of <0.05 was considered statistically significant.

3. Results

3.1. The Cytotoxicity of ADE. The MTT assay was used to evaluate the effect of ADE (0, 0.625, 1.25, 2.5, and 5 mM) on the cellular viabilities of HT22 cells. As shown in Figure 1(a), ADE exhibited cytotoxicity against HT22 cells in a dose-dependent manner. The cellular viabilities were decreased significantly after being exposed to ADE. As shown in Figure 1(b), the morphology of the HT22 cells has changed significantly characterized by cell shrinkage and irregular cell shapes. To further evaluate the effect of ADE-induced neurotoxicity, primary cultured cortical neuronal cells were treated with ADE (0, 1.25, 2.5, and 5 mM). As shown in Figure 1(c), ADE exhibited cytotoxicity against primary cultured cortical neuronal cells and the cellular viabilities were decreased significantly and dose-dependently after being exposed to ADE. As shown in Figure 1(d), primary cultured cortical neuronal cells exhibited obvious morphological changes characterized by shrinkage of neuronal cell bodies, reduction in the cell number and dendrites, and irregular cell shapes.

3.2. ADE Induces Apoptosis of HT22 Cells. HT22 cells were used to study whether ADE can induce apoptosis and the underlying mechanisms. As shown in Figure 2(a), after incubation with the ADE (0, 0.625, 1.25, and 2.5 mM) for 24 h, the morphological changes characterized by the nucleus pyknosis and fragmentation can be observed in

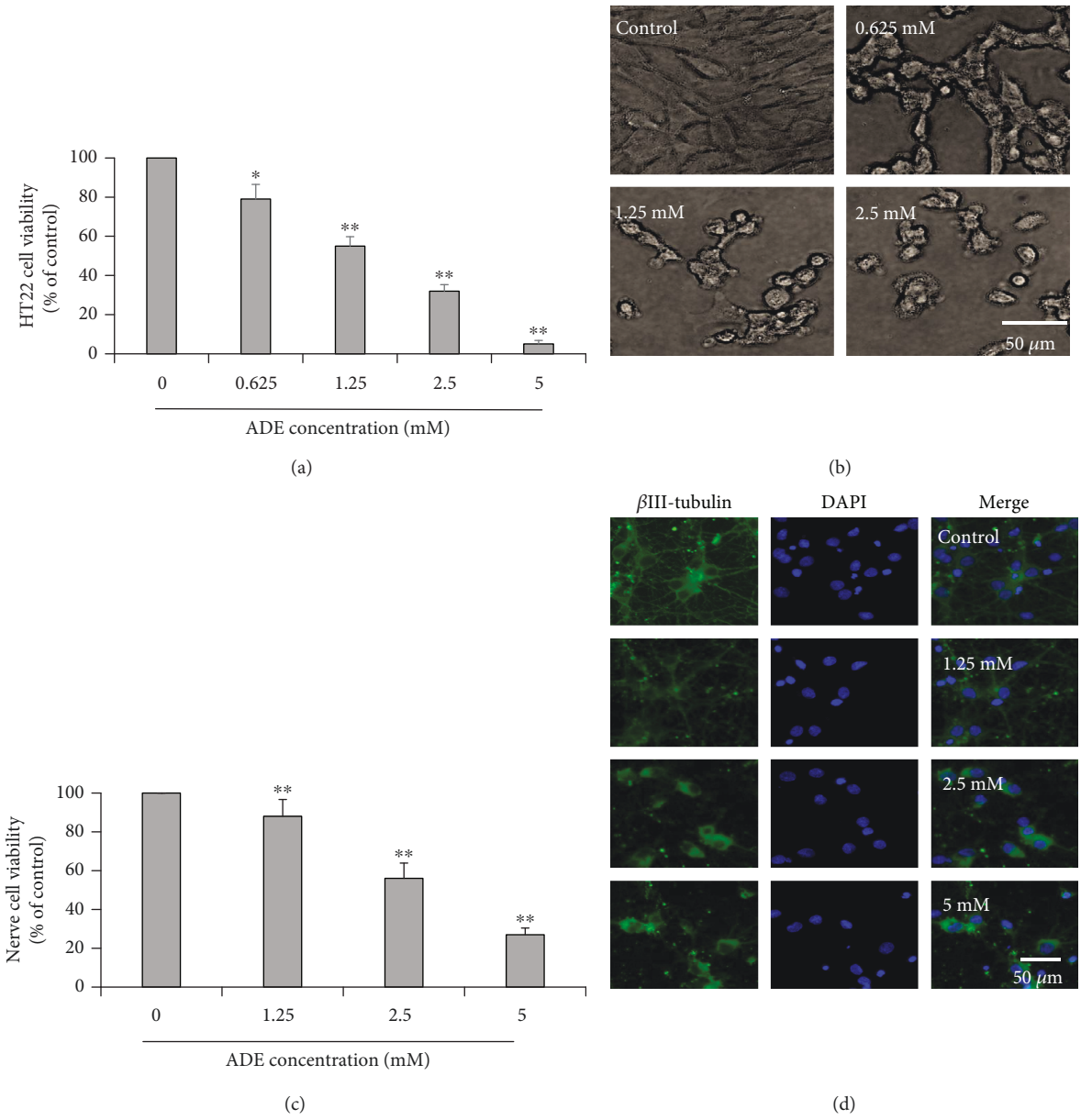

Figure 1: Effect of ADE on the cell viability and apoptosis of HT22 cells. Cells were incubated with various concentrations of ADE for 24 h. (a) Cell viability of HT22 cells after treatment with ADE (0, 0.625, 1.25, 2.5, and 5 mM). (b) Cellular morphology of HT22 cells after treatment with ADE (0, 0.625, 1.25, and 2.5 mM). (c) Cell viability of primary cultured cortical neuronal cells after treatment with ADE (0, 1.25, 2.5, and 5 mM). (d) Cellular morphology of primary cultured cortical neuronal cells stained with βIII-tubulin and DAPI after treatment with ADE (0, 1.25, 2.5, and 5 mM) ($n = 3$, $^{*}p < 0.05$, $^{**}p < 0.01$ vs the control group). One-way ANOVA followed by Dunnett's multiple comparison tests was used to detect significant differences from the control.

HT22 cells by Hoechst 33258 staining, indicating the appearance of apoptosis.

AO/EB staining was used to further distinguish the apoptosis of the cells. AO is a dye that penetrates normal cell membranes and causes cells to appear green in color. EB is a dye that passes through damaged cell membranes to cause cells to exhibit yellow fluorescence, demonstrating early apoptosis in cells. In our study, the nuclei of some cells appeared yellow or orange fluorescence after ADE treatment in Figure 2(b), which indicates that ADE disrupted the integrity of the cell membrane and might induce apoptosis in HT22 cells.

To clarify whether ADE induces apoptosis in HT22 cells, Annexin V-FITC/PI double-staining was used to measure the percentage of apoptotic cells in Figures 2(c) and 2(d). When compared with that in the control group, ADE treatment dose-dependently increased apoptotic ratio in HT22 cells. Therefore, these results suggest that ADE inhibited cell viabilities and induced apoptosis in HT22 cells.

Apoptosis-related proteins were further investigated to prove the ADE induced apoptosis. The data showed that the cleaved caspase-3, cleaved caspase-9, and cleaved caspase-12 expression levels were increased after ADE treatment in Figures 2(e) and 2(f). Treatment of HT22 cells with

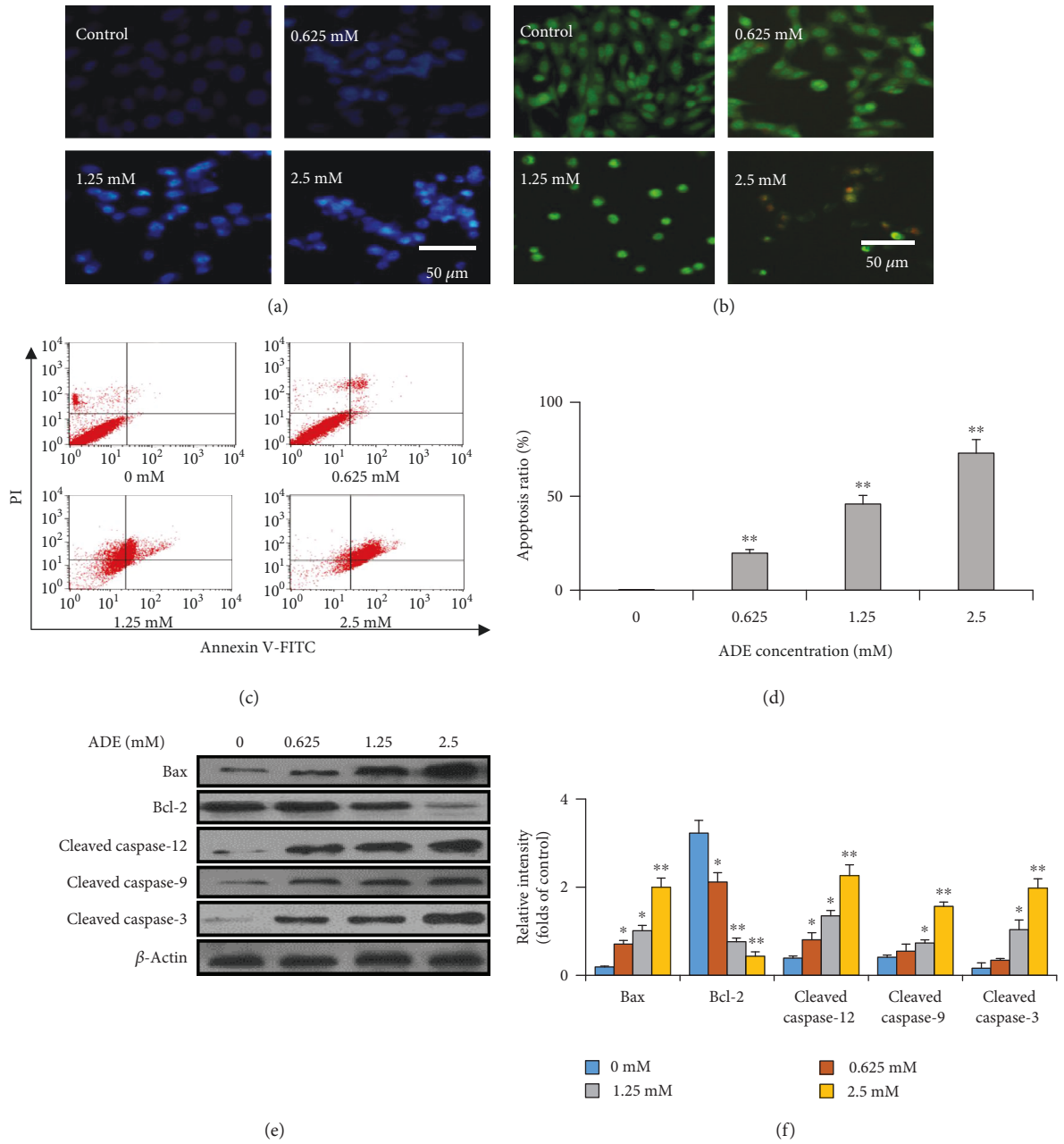

FIGURE 2: The exposure of ADE induces morphological changes of the HT22 cells. HT22 cells were incubated with ADE (0, 0.625, 1.25, and 2.5 mM) for 24 h, and then stained with Hoechst 33258 (a) and AO-EB (b), respectively. Scale bar = 50 μm. (c) Annexin V-FITC/PI double-staining of cells with ADE (0, 0.625, 1.25, and 2.5 mM) treatment for 24 h. (d) Quantified apoptotic rate ($n = 3$). (e) The expression levels of caspase family proteins, Bax and Bcl-2, by western blot. (f) Densitometric analysis of apoptosis-related proteins ($n = 3$, $^{*}p < 0.05$, $^{**}p < 0.01$ vs the control group). Statistical comparisons were made using one-way ANOVA with Dunnett's multiple comparison tests.

ADE also decreased intracellular Bcl-2 expression and increased Bax expression in Figures 2(e) and 2(f).

3.3. ADE Induces the ERS. In order to observe the changes of ER, TEM was used to directly observe the ultrastructural changes of ER after treatment with ADE (1.25 mM) for 24 h in HT22 cells. As shown in Figure 3(a), after treatment with ADE, the ER became swollen and vacuolated compared with the control group. In order to further prove the role of ERS in ADE-induced damage of HT22 cells, the expression levels of ERS-related mRNA were tested by RT-PCR. The data proved that the mRNA levels of GRP78, PERK, ATF6, caspase-12, and CHOP were dose-dependently upregulated in Figure 3(b).

Western blot was used to further demonstrate whether ERS is involved in cell apoptosis caused by ADE. As revealed in Figures 3(c) and 3(d), the protein expression levels of GRP78, ATF6, IRE1, p-IRE1, PERK, p-PERK, and CHOP were dose-dependently upregulated in the cells treatment with ADE. ERS-related CHOP protein was further detected

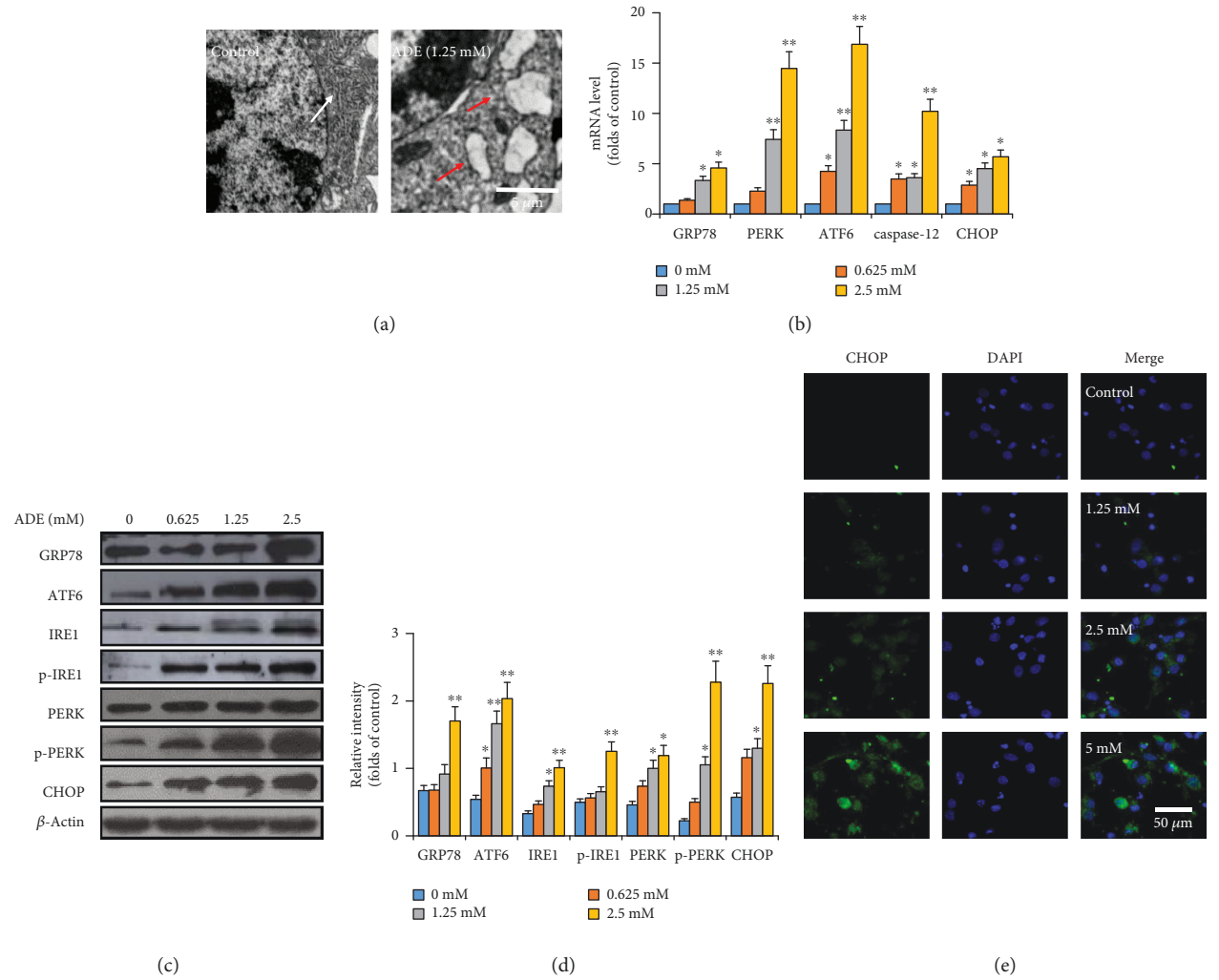

Figure 3: ADE induces ERS in HT22 cells. (a) Morphological changes of ER in HT22 cells after treatment with ADE were detected by TEM. The ER became swollen and vacuolated, as shown by red arrows. The white arrow indicates normal ER. (b) Effect of ADE on the mRNA levels of GRP78, PERK, ATF6, caspase-12, and CHOP in the HT22 cells. (c) After ADE treatment, the expression levels of GRP78, ATF6, IRE1, p-IRE1, PERK, p-PERK, and CHOP were elevated by western blot analysis. (d) ImageJ software was used to do the densitometric analysis of the ERS-related proteins. (e) Images of primary cultured cortical neuronal cells incubated with ADE for 24 h and stained with CHOP and DAPI. The targeted proteins were stained in green (CHOP), while the nuclei were stained in blue (DAPI) ($n = 3$, $^{*}p < 0.05$, $^{**}p < 0.01$ vs the control group). Statistical comparisons were made using one-way ANOVA with Dunnett's multiple comparison tests.

by immunofluorescence in primary cultured cortical neuronal cells. Our data showed that ADE upregulated CHOP expression in a dose-dependent manner in Figure 3(e).

3.4. ERS Contributes to ADE-Induced Overproduction of Intracellular Ca^{2+} and ROS. To further study the underlying mechanism of ADE-induced neurotoxicity, we tested the levels of ROS and Ca^{2+} in HT22 cells treated with ADE (0, 0.625, 1.25, and 2.5 mM) under a confocal microscope. The results showed that ADE treatment significantly increased intracellular ROS levels, indicating that ADE can induce oxidative stress in HT22 cells in Figures 4(a) and 4(b). Our data also demonstrated that ADE could significantly increase the intracellular Ca^{2+} levels Figures 4(c) and 4(d).

3.5. 4-PBA Attenuates ADE-Induced ERS and Apoptosis. To verify the role of ERS in HT22 cell apoptosis, HT22 cells were treated with ERS inhibitor 4-PBA (1.25 mM) for 2 h before treatment with ADE (1.25 mM) for 24 h. The MTT assay proved that 4-PBA mitigated ADE-induced cell viability decrease in Figure 5(a). The swollen and vacuolated ER induced by ADE was improved after treatment with 4-PBA (Figure 5(b)). 4-PBA pretreatment also reduced ADE-induced increase of CHOP, GRP78, ATF6, cleaved caspase-9, cleaved caspase-12, and cleaved caspase-3 levels in Figures 5(c) and 5(d).

3.6. NAC Attenuates ADE-Induced ERS and Apoptosis. Next, antioxidant NAC was used to further prove the role of oxidative stress in ERS-induced apoptosis. After pretreatment with NAC for 2 h, HT22 cells were treated with ADE (1.25 mM) for 24 h. As shown in Figure 6(a), the swollen and vacuolated ER induced by ADE was improved after pretreatment with NAC. We also proved that NAC reduced the accumulation

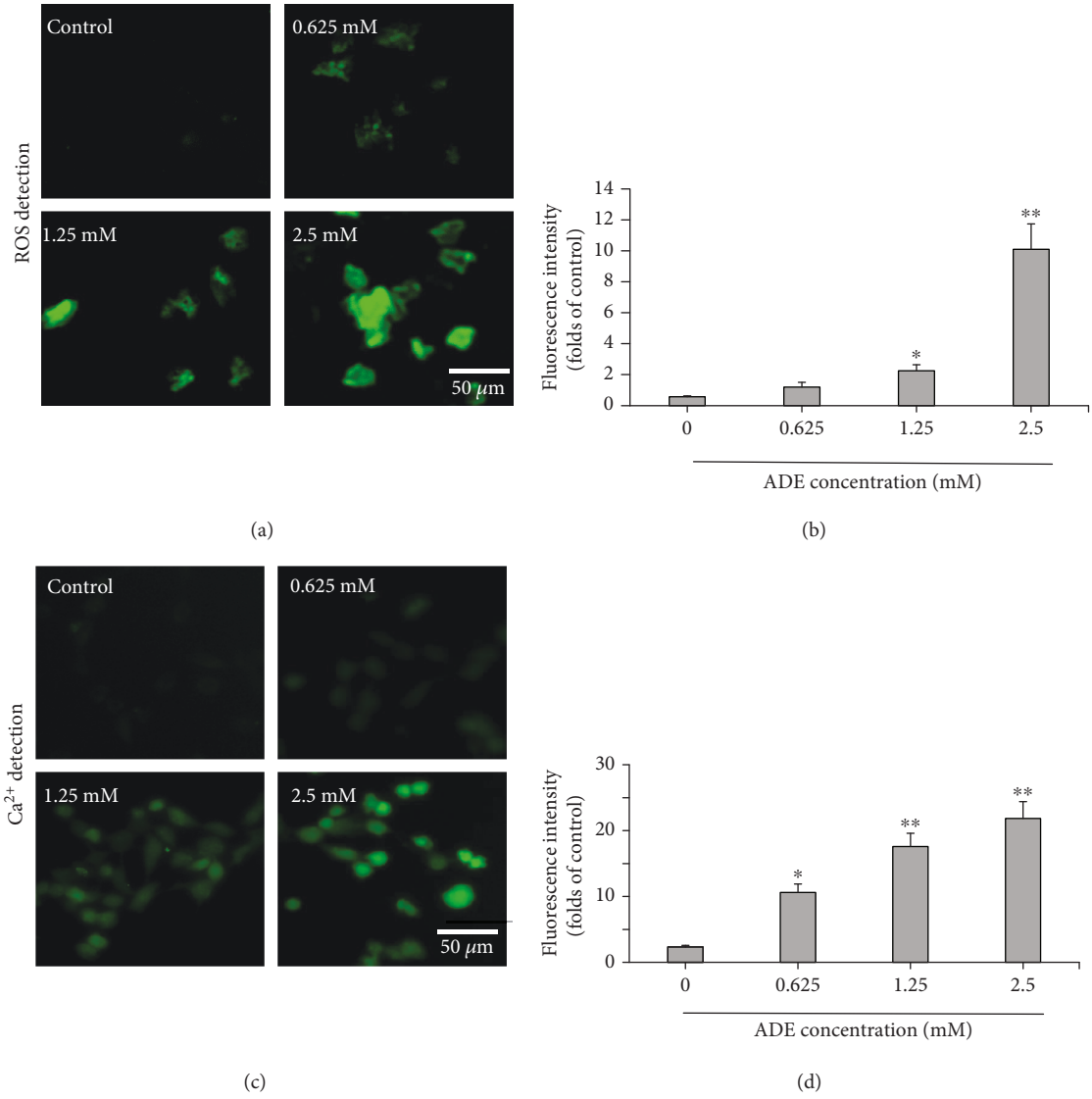

Figure 4: Changes of intracellular ROS and Ca^{2+} concentration in HT22 cells after treatment with ADE for 24 h. (a) DCFH-DA (green) was used to evaluate the intracellular ROS levels. The confocal microscope was used to take the fluorescence images. (b) ImageJ software was used to quantitatively analyze intracellular ROS levels in HT22 cells. (c) Representative images of Ca^{2+} levels in HT22 cell treatment with ADE under confocal microscopy. The levels of intracellular Ca^{2+} are indicated by green. (d) Quantitative analysis of representative intracellular Ca^{2+} levels in the control and ADE-treated HT22 cells by ImageJ software ($^{*}p < 0.05$, $^{**}p < 0.01$ vs the control group, $n = 3$). Statistical comparisons were made using one-way ANOVA with Dunnett's multiple comparison tests.

of ROS induced by ADE in HT22 cells in Figures 6(b) and 6(c). NAC pretreatment also reduced ADE-induced increase of CHOP, GRP78, ATF6, cleaved caspase-9, cleaved caspase-12, and cleaved caspase-3 levels in Figures 6(d) and 6(e).

4. Discussion

Excessive accumulation of ADE in the brain could lead to neurotoxicity and perhaps promote the development of neurodegenerative diseases [18]; however, the exact molecular mechanisms underlying ADE-induced neurotoxicity are not fully understood. Here, we studied the cytotoxic effects of ADE on HT22 cells and primary cultured cortical cells and found that ADE induced cytotoxicity by promoting apoptosis and inhibiting cell survival pathways.

Apoptosis is a programmed cell death that is usually caused by physiological or pathological factors. Evidence has shown that ADE is the most toxic metabolite of alcohol [4]. In various cell types, ADE is found to induce cytotoxicity and apoptosis [31, 32]. In this study, the destruction of the cell membrane integrity was demonstrated by staining the cells with AO/EB and Hoechst 33258. ADE was shown to induce apoptosis morphologically. Meanwhile, incubation with ADE caused obvious and dose-dependent increase of the percentage of dying cells by Annexin V-FITC/PI double-staining in HT22 cells, which was further proved in the primary cultured cortical cells. These results indicate that

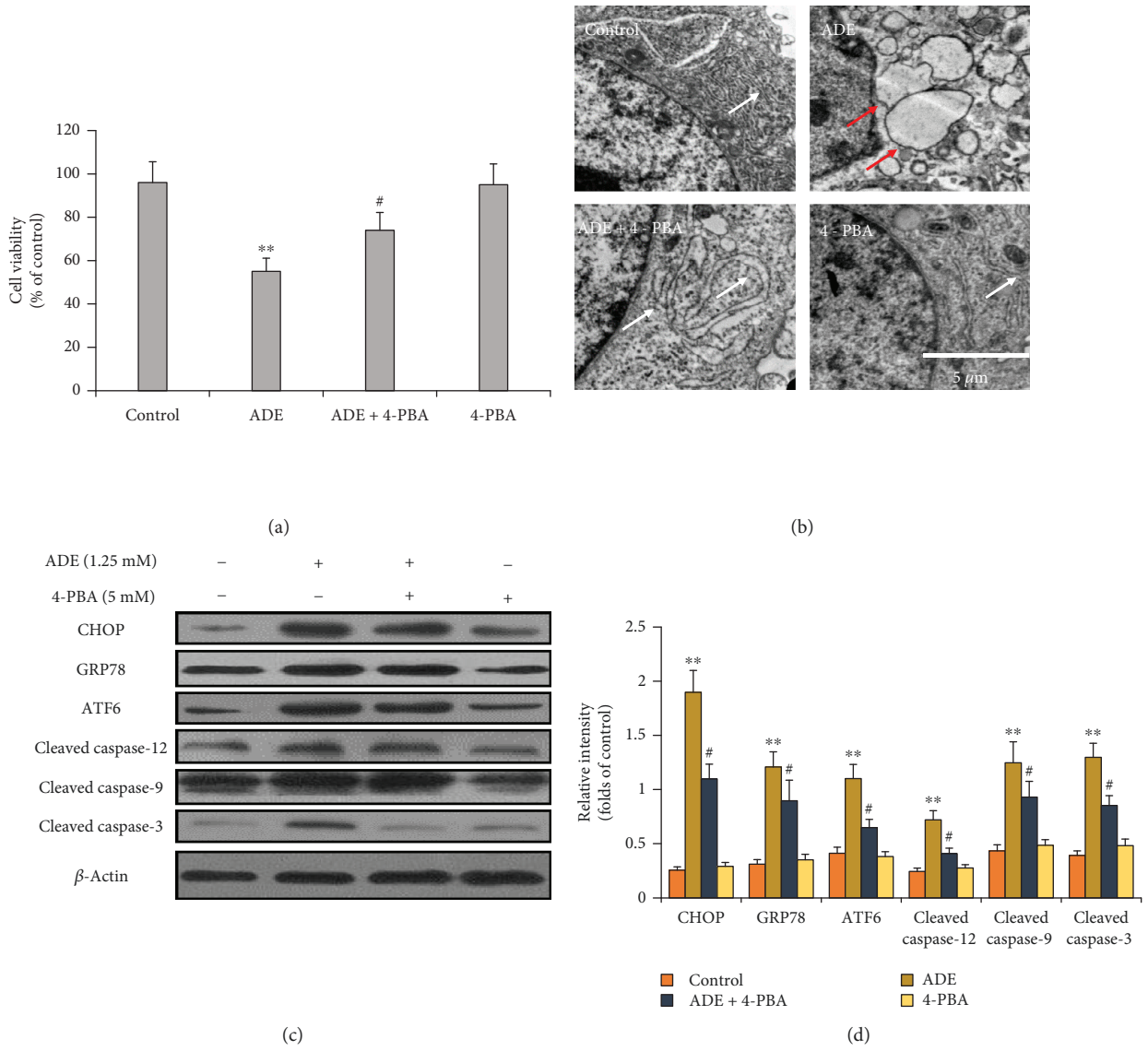

Figure 5: Effect of 4-PBA on ERS and apoptosis. (a) The MTT assay revealed that pretreatment with 4-PBA markedly inhibited ADE-induced cell viability decrease. (b) 4-PBA markedly improved ER morphological changes of HT22 cells after treatment with ADE. The red arrows indicate swollen and vacuolated ER, and the white arrows indicate normal ER. (c) Western blot analysis showed that 4-PBA markedly inhibited ADE-induced ERS- and apoptosis-related protein upregulation in HT22 cells. (d) Densitometric evaluation of western blot by ImageJ software ($n = 3$, $^{\#}p < 0.05$, ADE+4-PBA vs ADE; $^{**}p < 0.01$ ADE vs the HT22 control group). Statistical comparisons were made using one-way ANOVA with Dunnett's multiple comparison tests.

ADE induced cytotoxicity by inhibiting cell survival and promoting apoptosis.

Studies have shown that treatment with ADE leads to increase of intracellular ROS and oxidative stress *in vivo* [33]. ROS have close relationship with inflammation, oxidative stress, and cell damages [34, 35]. Previous investigations have shown that ADE can induce cytotoxicity by increasing the ROS accumulation and destroying redox homeostasis [3, 7]. In the current study, intracellular ROS levels were significantly increased by ADE treatment, suggesting that ADE can induce the oxidative stress by disrupting redox homeostasis in HT22 cells.

Ca^{2+} is an important second messenger that can participate in neurotransmitter release and signal transduction. Intracellular Ca^{2+} concentration changes can give rise to many cellular responses such as cell instability and cell damage [36]. At present, there is no literature on the relationship between ADE and Ca^{2+}. To explore the possible mechanism of ADE-induced HT22 cell injury, intracellular Ca^{2+} levels after ADE treatment were examined. The results demonstrated that ADE can significantly increase intracellular Ca^{2+} concentration, which might be related to the disrupted redox homeostasis and ultimately contribute to ADE-induced apoptosis in HT22 cells.

ER is an important organ regulating the intracellular environmental stability and is susceptible to oxidative stress [37]. In addition, ERS is closely related to the destruction of intracellular Ca^{2+} homeostasis. On the other hand, Ca^{2+} can

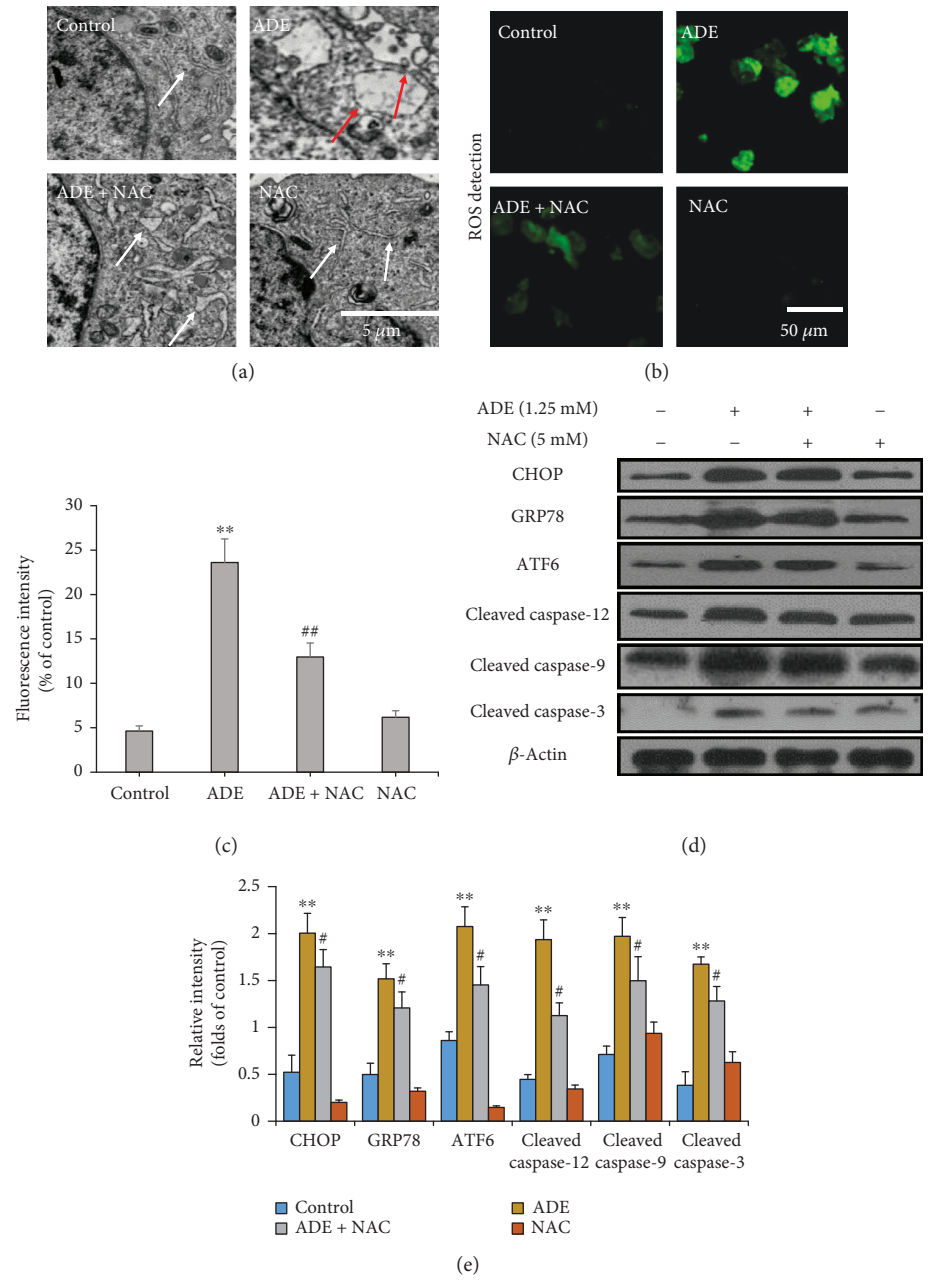

Figure 6: Effect of NAC on ERS and apoptosis. (a) NAC markedly improved HT22 cells' morphological changes of ER after treatment with ADE. The red arrows indicate swollen and vacuolated ER, and the white arrows indicate normal ER. (b) Fluorescence images of NAC pretreatment cells stained by DCFH-DA (green) were obtained by confocal microscope. (c) Quantitative analysis of ROS-positive cell percentages in each group by ImageJ software ($n = 3$, $^{\#\#}p < 0.01$, ADE+NAC vs ADE; $^{**}p < 0.01$ vs the HT22 control group). (d) Western blot analysis showed that NAC markedly inhibited ADE-induced ERS- and apoptosis-related protein upregulation in HT22 cells. (e) Densitometric evaluation of western blot by ImageJ software ($n = 3$, $^{\#}p < 0.05$, ADE+4-PBA vs ADE; $^{**}p < 0.01$ vs the HT22 control group). Statistical comparisons were made using one-way ANOVA with Dunnett's multiple comparison tests.

regulate the expression of ER molecular chaperones [38]. Therefore, we believed that the increased levels of intracellular ROS and Ca^{2+} might influence the function of ER (Figure 7).

Recent evidence indicates that ERS may play a role in the pathogenesis of neurological diseases [39] and has been implicated in various neurodegenerative processes, such as brain ischemia [40], Alzheimer's disease [41], Parkinson's disease [42], and amyotrophic lateral sclerosis [43]. The role of ER in the apoptotic process has been well established. ER apoptotic pathway is mainly regulated by activating GRP78, upregulating the expression of CHOP and cleave caspase-12, and inducing apoptosis [44]. The activation of ERS response or UPR is mediated mainly by 3 transmembrane ER signaling proteins: PERK, IRE1, and ATF6. In the current study, the mRNA levels of GRP78, PERK, ATF6,

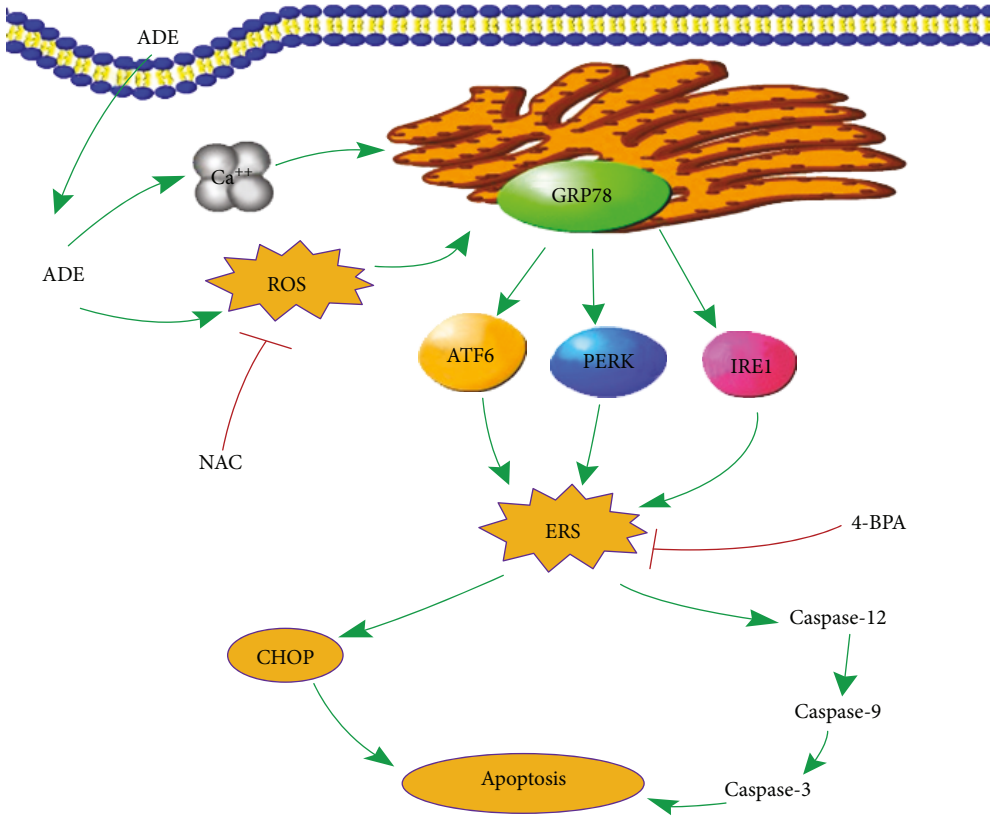

Figure 7: An illustration of the underlying mechanism of ADE-induced neurotoxicity.

CHOP, and caspase-12 were dose-dependently upregulated after ADE treatment. Furthermore, ERS-related proteins including IRE1, p-IRE1, ATF6, PERK, p-PERK, GRP78, and CHOP tested by western blot were also significantly upregulated after ADE treatment. The increase of PERK mRNA level is much more robust than the change of PERK protein, because PERK protein has been significantly phosphorylated to p-PERK after ADE treatment. Both PERK and IRE1 are type I transmembrane proteins of ER. PERK and IRE1 dissociate from the chaperone protein GRP78 when occurring ERS, forming phosphorylated forms of p-PERK and p-IRE1. In the present study, the protein levels of IRE1, p-IRE1, PERK, and p-PERK were all increased after ADE treatment, which strongly indicates the appearance of ERS.

To further examine ERS-mediated apoptosis, we tested the expression levels of CHOP and caspase-12. CHOP is a member of the bZIP transcription factor C/EBP family [39]. Under normal conditions, the expression level of CHOP is very low. When ERS occurs, the three main ERS pathways including IRE1, ATF6, and PERK can simultaneously stimulate CHOP [40, 41]. Caspase-12 is a unique endoplasmic reticulum apoptosis protease that can participate in ERS-induced apoptosis [42]. Our results suggest that following ADE treatment of HT22 cells, CHOP and cleaved caspase-12 levels were significantly increased, which were consistent with the changes at mRNA levels. We further measured CHOP protein in primary cultured cortical cells by immunofluorescence and showed that ADE obviously increased the expression of CHOP. These data indicate that ADE-induced apoptosis correlates with activated ERS sensors and upregulates ERS-related protein expression (Figure 7).

Basic and clinical studies over the past decade have shown that ROS have a significant impact on the pathogenesis of many human diseases [43]. In ERS, disorganized disulfide bond formation and disruption may lead to ROS accumulation and oxidative stress [44]. At the same time, ERS can cause mitochondrial damage and increase mitochondrial ROS production [45]. In addition, some UPR components such as CHOP may cause oxidative stress. In many *in vitro* and *in vivo* models related to ERS, ERS and oxidative stress emphasize each other in a positive feed-forward loop, which interferes with cell function and activates proapoptotic signaling [46]. In this study, the antioxidant NAC effectively inhibited the production of ROS and also alleviated the ERS (Figure 7). The results indicate that oxidative stress may promote ERS and induce cytotoxicity.

Here, for the first time, we proved that ADE induced neurotoxicity of HT22 cells via oxidative stress- and Ca^{2+} imbalance-mediated ERS. We explored the consequences of ADE on ER homeostasis and ROS production and found that ADE induced excessive generation of intracellular ROS and upregulation of ERS-related proteins GRP78, p-PERK, and p-IRE1. ER transmembrane proteins sense the folding state of proteins inside the ER lumen and convey the information to the mitochondria and the cytosol. 4-PBA, an ERS inhibitor, acts as a chemical chaperone assisting protein folding

in the ER as well as in the cytosol and the mitochondria [47]. In our results, inhibition of ROS with antioxidant NAC and mitigation of ERS with ERS inhibitor 4-PBA obviously suppressed ADE-induced apoptosis and the expression of ERS-related proteins. Meantime, we proved that antioxidant NAC not only mitigated ADE-induced ROS increase but also suppressed the swollen and vacuolated ER caused by ADE. Notably, the abnormal levels of ERS caused by ADE were significantly alleviated when ROS was inhibited by NAC. Therefore, on the basis of these findings, we believe that the activation of excessive ROS is a pathway contributing to the generation of ERS caused by ADE in the HT22 cells.

5. Conclusion

We demonstrated for the first time that ADE can cause neurotoxicity in HT22 cells and primary cultured cortical neuronal cells. ADE induced apoptosis of HT22 cells via the promotion of ERS, and excessive ROS and Ca^{2+} were involved in ADE-induced ERS. Our study also provides evidence that ERS inhibitor 4-PBA and antioxidant NAC may be beneficial for preventing neuronal damage associated with ADE-induced cytotoxicity which could be resulting from excessive alcohol consumption (Figure 7). Our data provides new insights into the underlying mechanisms of ADE-induced neurotoxicity. The ERS induced by ADE may have a profound effect on the CNS, which requires further study.

Abbreviations

ADE: Acetaldehyde
ADH: Alcohol dehydrogenase
ALDH: Aldehyde dehydrogenase
ERS: Endoplasmic reticulum stress
NAC: N-acetyl-L-cysteine
ROS: Reactive oxygen species
4-PBA: Sodium 4-phenylbutyrate.

Data Availability

The data used to support the findings of this study are available from the corresponding authors upon request.

Conflicts of Interest

The authors declare that there is no conflict of interests regarding the publication of this paper.

Acknowledgments

This study was supported by grants from the Program for Liaoning Excellent Talents in University (LJQ2015111), the National Natural Science Foundation of China (81403023), and the Natural Science Foundation of Liaoning Province of China (201602704).

References

[1] J. C. Brust, "Ethanol and cognition: indirect effects, neurotoxicity and neuroprotection: a review," *International Journal of Environmental Research and Public Health*, vol. 7, no. 4, pp. 1540–1557, 2010.

[2] Z. Guo and J. Li, "Chlorogenic acid prevents alcohol-induced brain damage in neonatal rat," *Translational Neuroscience*, vol. 8, pp. 176–181, 2017.

[3] T. Yan, Y. Zhao, X. Zhang, and X. Lin, "Astaxanthin inhibits acetaldehyde-induced cytotoxicity in SH-SY5Y cells by modulating Akt/CREB and p38MAPK/ERK signaling pathways," *Marine Drugs*, vol. 14, no. 3, 2016.

[4] C. Heit, H. Dong, Y. Chen, D. C. Thompson, R. A. Deitrich, and V. K. Vasiliou, "The role of CYP2E1 in alcohol metabolism and sensitivity in the central nervous system," in *Cytochrome P450 2E1: Its Role in Disease and Drug Metabolism*, vol. 67 of Sub-Cellular Biochemistry, , pp. 235–247, Springer, 2013.

[5] S. Gemma, S. Vichi, and E. Testai, "Individual susceptibility and alcohol effects: biochemical and genetic aspects," *Annali dell'Istituto Superiore di Sanità*, vol. 42, no. 1, pp. 8–16, 2006.

[6] G. S. Peng and S. J. Yin, "Effect of the allelic variants of aldehyde dehydrogenase *ALDH2*2* and alcohol dehydrogenase *ADH1B*2* on blood acetaldehyde concentrations," *Human Genomics*, vol. 3, no. 2, pp. 121–127, 2009.

[7] T. Yan, Y. Zhao, and X. Zhang, "Acetaldehyde induces cytotoxicity of SH-SY5Y cells via inhibition of Akt activation and induction of oxidative stress," *Oxidative Medicine and Cellular Longevity*, vol. 2016, Article ID 4512309, 9 pages, 2016.

[8] L. Martí-Prats, A. Orrico, A. Polache, and L. Granero, "Dual motor responses elicited by ethanol in the posterior VTA: consequences of the blockade of μ-opioid receptors," *Journal of Psychopharmacology*, vol. 29, no. 9, pp. 1029–1034, 2015.

[9] M. Melis, M. Diana, P. Enrico, M. Marinelli, and M. S. Brodie, "Ethanol and acetaldehyde action on central dopamine systems: mechanisms, modulation, and relationship to stress," *Alcohol*, vol. 43, no. 7, pp. 531–539, 2009.

[10] A. T. Peana, V. Porcheddu, F. Bennardini, A. Carta, M. Rosas, and E. Acquas, "Role of ethanol-derived acetaldehyde in operant oral self-administration of ethanol in rats," *Psychopharmacology*, vol. 232, no. 23, pp. 4269–4276, 2015.

[11] M. Tong, L. Longato, Q. G. L. Nguyen, W. C. Chen, A. Spaisman, and S. M. de la Monte, "Acetaldehyde-mediated neurotoxicity: relevance to fetal alcohol spectrum disorders," *Oxidative Medicine and Cellular Longevity*, vol. 2011, Article ID 213286, 13 pages, 2011.

[12] S. M. Zimatkin, S. P. Pronko, V. Vasiliou, F. J. Gonzalez, and R. A. Deitrich, "Enzymatic mechanisms of ethanol oxidation in the brain," *Alcoholism: Clinical and Experimental Research*, vol. 30, no. 9, pp. 1500–1505, 2006.

[13] M. Brandt and P. Wenzel, "Alcohol puts the heart under pressure: acetaldehyde activates a localized renin angiotensin aldosterone system within the myocardium in alcoholic cardiomyopathy," *International Journal of Cardiology*, vol. 257, pp. 220-221, 2018.

[14] A. T. Peana and E. Acquas, "Behavioral and biochemical evidence of the role of acetaldehyde in the motivational effects of ethanol," *Frontiers in Behavioral Neuroscience*, vol. 7, p. 86, 2013.

[15] A. T. Peana, M. Rosas, S. Porru, and E. Acquas, "From ethanol to salsolinol: role of ethanol metabolites in the effects of ethanol," *Journal of Experimental Neuroscience*, vol. 10, pp. 137–146, 2016.

[16] C. J. P. Eriksson, "The role of acetaldehyde in the actions of alcohol (update 2000)," *Alcoholism: Clinical and Experimental Research*, vol. 25, no. S1, pp. 15S–32S, 2001.

[17] G. A. Deehan Jr., S. R. Hauser, J. A. Wilden, W. A. Truitt, and Z. A. Rodd, "Elucidating the biological basis for the reinforcing actions of alcohol in the mesolimbic dopamine system: the role of active metabolites of alcohol," *Frontiers in Behavioral Neuroscience*, vol. 7, p. 104, 2013.

[18] X. S. Deng and R. Deitrich, "Putative role of brain acetaldehyde in ethanol addiction," *Current Drug Abuse Reviews*, vol. 1, no. 1, pp. 3–8, 2008.

[19] M. Salaspuro, "Acetaldehyde and gastric cancer," *Journal of Digestive Diseases*, vol. 12, no. 2, pp. 51–59, 2011.

[20] E. M. Tacconi, X. Lai, C. Folio et al., "BRCA1 and BRCA2 tumor suppressors protect against endogenous acetaldehyde toxicity," *EMBO Molecular Medicine*, vol. 9, no. 10, pp. 1398–1414, 2017.

[21] A. A. Mansoori and S. K. Jain, "ADH1B, ALDH2, GSTM1 and GSTT1 gene polymorphic frequencies among alcoholics and controls in the Arcadian population of Central India," *Asian Pacific Journal of Cancer Prevention*, vol. 19, no. 3, pp. 725–731, 2018.

[22] D. J. Tuma, "Role of malondialdehyde-acetaldehyde adducts in liver injury," *Free Radical Biology & Medicine*, vol. 32, no. 4, pp. 303–308, 2002.

[23] D. J. Tuma and C. A. Casey, "Dangerous byproducts of alcohol breakdown—focus on adducts," *Alcohol Research & Health*, vol. 27, no. 4, pp. 285–290, 2003.

[24] G. Rathnasamy, M. Murugan, E. A. Ling, and C. Kaur, "Hypoxia-induced iron accumulation in oligodendrocytes mediates apoptosis by eliciting endoplasmic reticulum stress," *Molecular Neurobiology*, vol. 53, no. 7, pp. 4713–4727, 2016.

[25] V. Rubovitch, S. Barak, L. Rachmany, R. B. Goldstein, Y. Zilberstein, and C. G. Pick, "The neuroprotective effect of salubrinal in a mouse model of traumatic brain injury," *Neuromolecular Medicine*, vol. 17, no. 1, pp. 58–70, 2015.

[26] F. Yang and J. Luo, "Endoplasmic reticulum stress and ethanol neurotoxicity," *Biomolecules*, vol. 5, no. 4, pp. 2538–2553, 2015.

[27] X. Lu, R. R. Yang, J. L. Zhang et al., "Tauroursodeoxycholic acid produces antidepressant-like effects in a chronic unpredictable stress model of depression via attenuation of neuroinflammation, oxido-nitrosative stress and endoplasmic reticulum stress," *Fundamental & Clinical Pharmacology*, vol. 32, no. 4, pp. 363–377, 2018.

[28] G. Chen, C. Ma, K. A. Bower, X. Shi, Z. Ke, and J. Luo, "Ethanol promotes endoplasmic reticulum stress-induced neuronal death: involvement of oxidative stress," *Journal of Neuroscience Research*, vol. 86, no. 4, pp. 937–946, 2008.

[29] A. C. A. Oliveira, M. C. S. Pereira, L. N. . S. Santana et al., "Chronic ethanol exposure during adolescence through early adulthood in female rats induces emotional and memory deficits associated with morphological and molecular alterations in hippocampus," *Journal of Psychopharmacology*, vol. 29, no. 6, pp. 712–724, 2015.

[30] D. Zuo, F. Sun, J. Cui et al., "Alcohol amplifies ketamine-induced apoptosis in primary cultured cortical neurons and PC12 cells through down-regulating CREB-related signaling pathways," *Scientific Reports*, vol. 7, no. 1, article 10523, 2017.

[31] E. Elamin, A. Masclee, F. Troost, J. Dekker, and D. Jonkers, "Cytotoxicity and metabolic stress induced by acetaldehyde in human intestinal LS174T goblet-like cells," *American Journal of Physiology-Gastrointestinal and Liver Physiology*, vol. 307, no. 3, pp. G286–G294, 2014.

[32] Y. Liu, M. Yamanaka, N. Abe-Kanoh et al., "Benzyl isothiocyanate ameliorates acetaldehyde-induced cytotoxicity by enhancing aldehyde dehydrogenase activity in murine hepatoma Hepa1c1c7 cells," *Food and Chemical Toxicology*, vol. 108, Part A, pp. 305–313, 2017.

[33] C. R. Goodlett, K. H. Horn, and F. C. Zhou, "Alcohol teratogenesis: mechanisms of damage and strategies for intervention," *Experimental Biology and Medicine*, vol. 230, no. 6, pp. 394–406, 2005.

[34] K. Buyukhatipoglu and A. M. Clyne, "Superparamagnetic iron oxide nanoparticles change endothelial cell morphology and mechanics via reactive oxygen species formation," *Journal of Biomedical Materials Research Part A*, vol. 96A, no. 1, pp. 186–195, 2011.

[35] S. Naqvi, M. Samim, M. Abdin et al., "Concentration-dependent toxicity of iron oxide nanoparticles mediated by increased oxidative stress," *International Journal of Nanomedicine*, vol. 5, pp. 983–989, 2010.

[36] J. J. Palop and L. Mucke, "Amyloid-β–induced neuronal dysfunction in Alzheimer's disease: from synapses toward neural networks," *Nature Neuroscience*, vol. 13, no. 7, pp. 812–818, 2010.

[37] J. D. Malhotra, H. Miao, K. Zhang et al., "Antioxidants reduce endoplasmic reticulum stress and improve protein secretion," *Proceedings of the National Academy of Sciences of the United States of America*, vol. 105, no. 47, pp. 18525–18530, 2008.

[38] C. Xu, B. Bailly-Maitre, and J. C. Reed, "Endoplasmic reticulum stress: cell life and death decisions," *The Journal of Clinical Investigation*, vol. 115, no. 10, pp. 2656–2664, 2005.

[39] A. Canales, M. Rösinger, J. Sastre et al., "Hidden α-helical propensity segments within disordered regions of the transcriptional activator CHOP," *PLoS One*, vol. 12, no. 12, article e0189171, 2017.

[40] Y. Adachi, K. Yamamoto, T. Okada, H. Yoshida, A. Harada, and K. Mori, "Atf6 is a transcription factor specializing in the regulation of quality control proteins in the endoplasmic reticulum," *Cell Structure and Function*, vol. 33, no. 1, pp. 75–89, 2008.

[41] S. Oyadomari and M. Mori, "Roles of CHOP/GADD153 in endoplasmic reticulum stress," *Cell Death & Differentiation*, vol. 11, no. 4, pp. 381–389, 2004.

[42] I. Moserova and J. Kralova, "Role of ER stress response in photodynamic therapy: ROS generated in different subcellular compartments trigger diverse cell death pathways," *PLoS One*, vol. 7, no. 3, article e32972, 2012.

[43] S. Wang and R. J. Kaufman, "The impact of the unfolded protein response on human disease," *The Journal of Cell Biology*, vol. 197, no. 7, pp. 857–867, 2012.

[44] S. S. Cao and R. J. Kaufman, "Endoplasmic reticulum stress and oxidative stress in cell fate decision and human disease," *Antioxidants & Redox Signaling*, vol. 21, no. 3, pp. 396–413, 2014.

[45] H. F. Wang, Z. Q. Wang, Y. Ding et al., "Endoplasmic reticulum stress regulates oxygen-glucose deprivation-induced

parthanatos in human SH-SY5Y cells via improvement of intracellular ROS," *CNS Neuroscience & Therapeutics*, vol. 24, no. 1, pp. 29–38, 2018.

[46] J. D. Malhotra and R. J. Kaufman, "Endoplasmic reticulum stress and oxidative stress: a vicious cycle or a double-edged sword?," *Antioxidants & Redox Signaling*, vol. 9, no. 12, pp. 2277–2294, 2007.

[47] Y. P. Hong, W. H. Deng, W. Y. Guo et al., "Inhibition of endoplasmic reticulum stress by 4-phenylbutyric acid prevents vital organ injury in rat acute pancreatitis," *American Journal of Physiology-Gastrointestinal and Liver Physiology*, vol. 315, no. 5, pp. G838–G847, 2018.